I&EC research
Industrial & Engineering Chemistry Research

Article

Prediction of Phase Behaviors of Polymer Solvent Mixtures from the COSMO-SAC Activity Coefficient Model

Yu-Ching Kuo, Chan-Chia Hsu, and Shiang-Tai Lin

Ind. Eng. Chem. Res., **Just Accepted Manuscript** • DOI: 10.1021/ie402175k • Publication Date (Web): 22 Aug 2013

Industrial & Engineering Chemistry Research is published by the American Chemical Society. 1155 Sixteenth Street N.W., Washington, DC 20036

Prediction of Phase Behaviors of Polymer Solvent Mixtures from the COSMO-SAC Activity Coefficient Model

*Yu-Ching Kuo†, Chan-Chia Hsu† and Shiang-Tai Lin**

Department of Chemical Engineering, National Taiwan University, Taipei, Taiwan

*To whom correspondence should be addressed: Email: stlin@ntu.edu.tw

†Both authors contributed equally to this work.

Abstract

An efficient method for prediction of the vapor-liquid and liquid-liquid phase behaviors of polymer solvent mixtures is proposed using the COSMO-SAC activity coefficient model. In particular, we examine various approaches for generating the screening charge distribution of homepolymers and copolymers from quantum mechanical calculations and propose a novel method to generate such data efficiently using a finite number of repeating units. The free volume effects known to be important in polymer solutions are considered through the free volume model of Elbro and coworkers. We have examined this model using 2249 vapor-liquid equilibria data points from 25 homopolymers, 8 copolymers and 48 solvents. The overall average deviation (AAD%) of solvent activity is found to be about 16%, which is comparable to that from other UNIFAC-based models. The liquid-liquid equilibrium of polymer solvent mixtures can be predicted in qualitative agreement with experiment. The proposed method is capable of describing the changes in solvent activity due to temperature, polymer molecular weight, and polymer tacticity. Our results suggest that the proposed method is a useful complementary to group contribution method for phase behavior of polymer solutions when group parameter or density information of polymers is unavailable.

Keywords: COSMO-SAC; Vapor-Liquid Equilibrium; Polymer Solutions; Tacticity; Solvent Activity;

1. Introduction

Polymers are used extensively in our daily life because of their diverse and adjustable material properties. The properties of a polymer can be altered by changing its chemical composition, its molecular weight, tacticity, introducing different side chains, or addition of other chemicals. The knowledge of phase behavior of a polymer is critical for polymer processing such as synthesis, polymerization and separation of solvents from polymer solutions.[1-3]

Many efforts have been made for the modeling of phase behaviors of polymer solutions. One class of methods focuses on the description of pressure-volume-temperature-composition equation of state of polymer solutions, such as the group contribution-parameter EOS,[4-13] SAFT-based EOS[14-16] and cubic EOS.[17-28] While such EOS provides complete thermodynamic information of the polymer solutions, they often contain parameters for both the polymer itself and polymer-solvent interactions that need to be determined with appropriate experimental data. Although group contribution EOS has the great ability to predict the phase diagram of polymer solutions based on exist functional group parameters, it sometimes suffers from missing parameter. Another class of methods focuses on the modeling of the excess Gibbs free energy of the solution, such as the Flory-Huggins (FH) model[29-31] and the extension of activity coefficient models for ordinary liquids, such as the group contribution UNIFAC model.[32] One important difference between ordinary mixtures and mixtures containing polymers is the non-negligible change of free volume (FV)[33, 34] upon mixing. For example, Oishi et al.[32] developed a free volume term for UNIFAC model and Entropic-FV[35] models adopted the free volume term developed by Elbro et al.[36] Recently, many improvements[37-41] are proposed based on the above two activity coefficient models by modifying the free volume term and group interaction

parameters. Comparison of the performance of different methods in vapor-liquid equilibrium (VLE) of polymer solutions can be found by the work of Costa et al.[42] Kontogeorgis et al.[43] and Bogdanic et al.[44] summarized the performance of several predictive group contributions models for the liquid-liquid equilibrium (LLE) prediction in polymer solutions. The group contribution based methods are predictive when all the group interaction parameters are available. For polymers containing multifunctional groups, it is likely that not all needed parameters are readily available.

Recently, Yang et al.[45] demonstrated the successful predictions of VLE of polymer solutions without use of any parameters based on the COSMO-SAC model.[46-48] This is possible because the molecular information and molecular interactions were determined from the results of quantum mechanical (QM) calculations. However, due to high computational demands in QM calculations for polymers, only 5 homopolymers were considered. In this work, we present a new, efficient method to generate the input for COSMO-SAC model for both homopolymers and copolymers based on QM calculations. Furthermore, the free volume term proposed by Elbro et al. is included in COSMO-SAC model. The inclusion of free volume effects significantly improves the model accuracy in both VLE and LLE predictions. The proposed method thus provides a more viable and efficient approach for the prediction of phase behaviors of polymer solutions when no experimental data is available.

2. Theories

2.1 The criteria for phase equilibrium

When a vapor-liquid or liquid-liquid system reaches equilibrium, the chemical potential (or fugacity) of each component in different phases must be the same, i.e.,

$$\bar{f}_i^I(T,P,\underline{x}^I) = \bar{f}_i^{II}(T,P,\underline{x}^{II}) \quad (1)$$

where the superscripts I and II denote the phases; f_i is the fugacity of species i, and $\underline{x}$ represents the molar composition of the phase.

For vapor-liquid equilibrium of polymer solvent mixture at conditions remote from the critical point of the solvent (so that the vapor phase is ideal) can be determined from the equality of solvent fugacity in the vapor and liquid phases, i.e.,

$$x_{solvent}^V P = x_{solvent}^L \gamma_{solvent} P_{solvent}^{vap} \quad (2)$$

where P_i^{vap} is the pure vapor pressure of species i at the same temperature, and γ_i is the activity coefficient of i calculated by a liquid model. Note that for a binary mixture (polymer+solvent) the vapor phase is pure solvent ($x_{solvent}^V = 1$). For liquid-liquid equilibrium, the equilibrium composition can be determined from the knowledge of activity coefficient as

$$x_i^I \gamma_i^I = x_i^{II} \gamma_i^{II} \quad (3)$$

Therefore, the activity coefficient of solvent and polymer in the liquid phase is the key property in both VLE and LLE calculations.

2.2 The COSMO-SAC model

In this work, the activity coefficient is determined from the COSMO-SAC model,[49] where the activity coefficient $\gamma_{i/s}$ of solute i in the solution s can be represented as following equation:

$$ln\,\gamma_{i/s} = ln\,\gamma_{i/s}^{res} + ln\,\gamma_{i/s}^{comb} \quad (4)$$

where the superscript res and comb represent residual and combinatorial contributions, respectively. The combinatorial term is used to represent the difference of molecular size and shape between the species. In COSMO-SAC model, the Staverman-Guggenheim combinatorial term[50] is used:

$$ln\,\gamma_{i/s}^{comb} = ln\frac{\phi_i}{x_i} + \frac{z}{2}q_i\,ln\frac{\theta_i}{\phi_i} + I_i - \frac{\phi_i}{x_i}\sum_j x_j I_j \tag{5}$$

where ϕ_i, θ_i and x_i are the surface fraction, the volume fraction and mole fraction of component i respectively,

$$\phi_i = \frac{x_i q_i}{\sum_j x_j q_j};\ \theta_i = \frac{x_i r_i}{\sum_j x_j r_j};\ I_j = \frac{z}{2}\left(r_i - q_i\right) - \left(r_i - l\right) \tag{6}$$

with z being the coordination number (taken to be 10). The r_i and q_i are normalized volume and surface area parameters of component i

$$r_i = \frac{V_i^{cosmo}}{r};\ q_i = \frac{A_i^{cosmo}}{q} \tag{7}$$

where r=66.69 Å^3 and q=79.53 Å^2.[48]

The residual contribution to the activity coefficient is determined from the difference of the restoring solvation free energy of component i in the solution ($\Delta\underline{G}_{i/s}^{*res}$) and in its pure liquid,

$$ln\,\gamma_{i/s}^{residual} = \frac{\Delta\underline{G}_{i/s}^{*res} - \Delta\underline{G}_{i/i}^{*res}}{RT} \tag{8}$$

Molecules in the liquid phase are considered in close contact and the restoring free energy is determined by considering the ensemble of surface interactions at different contacting configurations. The surface interactions are estimated from the molecular surface screening charges calculated when the molecule is embedded in a perfect conductor.[51, 52] These surface charges are averaged to obtain apparent screening charges to be used in COSMO-SAC model according to

$$\sigma_m = \frac{\sum_n \sigma_n^* \frac{r_n^2 r_{eff}^2}{r_n^2 + r_{eff}^2} exp\left(-f_{decay} \frac{d_{mn}^2}{r_n^2 + r_{eff}^2}\right)}{\sum_n \frac{r_n^2 r_{eff}^2}{r_n^2 + r_{eff}^2} exp\left(-f_{decay} \frac{d_{mn}^2}{r_n^2 + r_{eff}^2}\right)} \tag{9}$$

where σ_n^* and σ_m are charge densities before and after charge averaging; the subscripts m and n represent segments m and n respectively; $r_n = \sqrt{a_n / \pi}$ is the radius of segment; $r_{eff} = \sqrt{a_{eff} / \pi}$ is the radius of a standard surface segment; the f_{decay} is an empirical parameter whose value is 3.57,[53] and d_{mn} is the distant between segment m and n. The three-dimensional screening charge is quantified to a histogram, known as the σ-profile, p(σ), which represents the probability of finding a segment with screening charge density σ,

$$p_i(\sigma_m) = \frac{A_i(\sigma_m)}{A_i} \tag{10}$$

where $A_i(\sigma_m)$ is the segment surface area with screening charge density σ_m and A_i is the total surface area of component *i*. For a better description of hydrogen-bonding interactions, Hsieh et al.[49] further classified the molecular surface into hydrogen-bonding $A_i^{hb}(\sigma_m)$ and non-hydrogen-bonding $A_i^{nhb}(\sigma_m)$ parts. The hydrogen-bonding part was separated into hydroxyl hydrogen-

bonding $A_i^{OH}(\sigma_m)$ (e.g., OH in water and alcohol) and other hydrogen-bonding $A_i^{OT}(\sigma_m)$ (e.g., O in ketones, NH_2 in amines) contributions. Thus, the σ-profile becomes:

$$p_i^t(\sigma_m) = \frac{A_i^t(\sigma_m^t)}{A_i} f^t(\sigma_m) \tag{11}$$

where superscript t takes the value of *nhb*, *OH*, or *OT*, and the function *f(t)* provides a Gaussian-type screening for hydrogen bonding surfaces

$$f^t(\sigma_m) = \begin{cases} 1 - \left(exp \frac{\sigma_m^2}{2\sigma_0^2} \right) & for\ t = OH, OT \\ \left(exp \frac{\sigma_m^2}{2\sigma_0^2} \right) & for\ t = nhb \end{cases} \tag{12}$$

with σ_0 being a constant of 0.007e/Å^2.[54] For a mixture the σ-profile is calculated from the area weighted average of contributions from all its components as

$$p_s^t(\sigma_m^t) = \frac{\sum_i x_i A_i p_i(\sigma_m^t)}{\sum_i x_i A_i} \tag{13}$$

The activity coefficient of surface type *t* with a charge density of σ_m is determined in the following equation:

$$ln\,\Gamma_j^t(\sigma_m^t) = -ln \sum_s^{hb,OH,OT} \sum_{\sigma_n} p_j^s(\sigma_n^s) \Gamma_j^t(\sigma_n^s) exp\left[\frac{-\Delta W(\sigma_m^t, \sigma_n^s)}{RT} \right] \tag{14}$$

where subscript *j* can be either pure liquid or mixture; The superscripts *s* and *t* represent the property for hydrogen-bonding or non-hydrogen-bonding surface segments. The exchange energy in the above equation can be determined as:

$$\Delta W\left(\sigma_m^t,\sigma_n^s\right)=c_{ES}\left(\sigma_m^t+\sigma_n^s\right)^2-c_{hb}\left(\sigma_m^t,\sigma_n^s\right)\left(\sigma_m^t-\sigma_n^s\right)^2 \tag{15}$$

The c_{ES} is an electrostatic interaction parameter which is dependent on temperature.

$$c_{ES}=A_{ES}+\frac{B_{ES}}{T^2} \tag{16}$$

both A_{ES} and B_{ES} are universal parameters, 6525.69 (kcal/mol)(A^4/e^2) and 1.4859×10^8 (kcal/mole)(A^4/e^2)K^2, respectively.[49] The hydrogen-bonding interaction parameter $c_{hb}\left(\sigma_m^t,\sigma_n^s\right)$ is defined as the following:

$$c_{hb}\left(\sigma_m^t,\sigma_n^s\right)=\begin{cases}c_{OH-OH} & if\ s=t=OH\ and\ \sigma_m^t\cdot\sigma_n^s<0\\ c_{OT-OT} & if\ s=t=OT\ and\ \sigma_m^t\cdot\sigma_n^s<0\\ c_{OT-OH} & if\ s=OH,t=OH,and\ \sigma_m^t\cdot\sigma_n^s<0\\ 0 & Otherwise\end{cases} \tag{17}$$

The values of $c_{OH\text{-}OH}$, $c_{OT\text{-}OT}$ and $c_{OT\text{-}OH}$ were obtained from regression to experimental data, and determined to be 4013.78 (kcal/mol)(A^4/e^2), 932.31 (kcal/mol)(A^4/e^2) and 3016.43 (kcal/mol)(A^4/e^2), respectively.[49] The restoring solvation free energy can then be obtained from the segment activity coefficient as

$$\frac{\Delta G_{i/j}^{*res}}{RT}=\frac{A_i}{a_{eff}}\sum\nolimits_s^{nhb,hb}\sum_{\sigma_m}p_i^s\left(\sigma_m^s\right)ln\,\Gamma_j^s\left(\sigma_m^s\right) \tag{18}$$

Equation 18 is used in eq.8 for the residual component of the activity coefficient.

It can be seen (in eqs. 8, 14, and 18) that the σ-profile, the screening charge density distribution, is the most important molecular information in the COSMO-SAC model. For small molecules such information can be obtained directly from DFT/COSMO calculations.[51] However, for polymers it is too computationally costly to be done for each specific case (note that the computational time increases with the number of electrons contained in the molecule to the 3rd or 4th power). Therefore, it is not practical to perform DFT/COSMO calculations on the real polymer structures. Here we propose to determine the σ-profile of a polymer of any desired chain length from its oligomer.

For a homopolymer from the DFT/COSMO calculation is performed on its tri-mer with the two ends capped with CH3 or hydrogen atoms. Once the charge averaging (eq. 9) is done, the surface area and charge of segments belonging to middle unit of the tri-mer are multiplied by N_{units}-2 times in order to generate the 鴉-profile of polymer of degree of polymerization N_{units}. All subsequent calculations follow the standard procedure (as described in the following section). Figure 1(a) and 1(b) illustrate the σ-profile of a PVOH tri-mer and the middle unit of PVOH. By multiplying the area and charge of segments of the middle unit of tri-mer, the σ-profile of polymer PVOH is obtained (see Figure 1(c)).

For a copolymer, the DFT/COSMO calculation is performed on the tetra-mer. Two kinds of arrangements for repeating units A and B are examined in this work: A-B-A-B and A-A-B-B. The surface area and charge of segments belonging to the middle repeating unit A of a tetra-mer is multiplied by $N_{units,A}$-1 and B is multiplied by $N_{units,B}$-1. Where the $N_{units,A}$ and $N_{units,B}$ denote the degree of polymerization of the monomer A and B in a copolymer structure respectively.

The molecular volume and surface area needed for the combinatorial term (eq. 7) can also be estimated from those of tri-mers and tetra-mers. The homopolymer surface area and

volume denoted as A_{hp}^{cosmo} and V_{hp}^{cosmo}; the copolymer surface area and volume are A_{cp}^{cosmo} and V_{cp}^{cosmo}. These values can be estimated from the following equations:

$$A_{hp}^{cosmo} = A_m^{cosmo} \cdot (N_{units} - 2) + (A_{trimer}^{cosmo} - A_m^{cosmo}) \quad (19)$$

$$V_m^{cosmo} = \frac{A_m^{cosmo}}{A_{trimer}^{cosmo}} \cdot V_{trimer}^{cosmo} \quad (20)$$

$$V_{hp}^{cosmo} = V_m^{cosmo} \cdot N_{units} \quad (21)$$

$$A_{cp}^{cosmo} = A_A^{cosmo} \cdot (N_{units,A} - 1) + A_B^{cosmo} \cdot (N_{units,B} - 1) + (A_{tetramer}^{cosmo} - A_A^{cosmo} - A_B^{cosmo}) \quad (22)$$

$$V_A^{cosmo} = \frac{A_A^{cosmo}}{A_{tetramer}^{cosmo}} \cdot V_{tetramer}^{cosmo} \quad (23)$$

$$V_B^{cosmo} = \frac{A_B^{cosmo}}{A_{tetramer}^{cosmo}} \cdot V_{tetramer}^{cosmo} \quad (24)$$

$$V_{cp}^{cosmo} = V_A^{cosmo} \cdot N_{units,A} + V_B^{cosmo} \cdot N_{units,B} \quad (25)$$

where A_m^{cosmo} and V_m^{cosmo} are the total surface area and volume of the middle unit of a tri-mer; A_A^{cosmo} and V_A^{cosmo} are the total surface area and volume of the monomer A while subscript B represents the monomer B in a copolymer structure. A_{trimer}^{cosmo}, V_{trimer}^{cosmo}, $A_{tetramer}^{cosmo}$ and $V_{tetramer}^{cosmo}$ are the area and volume of the tri-mer and tetramer, which can be obtained directly from the output of DFT/COSMO calculation. With this procedure, we can generate the σ-profile of any desired molecular weight within a second once the DFT/COSMO calculation is performed for the tri-mer and tetra-mer of the polymers.

2.3 Modification of COSMO-SAC to include free-volume effects

The change in free volume in polymer solutions has been shown to have a significant impact on the phase behaviors.[33, 34] In this work the free volume term proposed by Elbro et al[36] is introduced into COSMO-SAC model to replace the original Staverman-Guggenheim combinatorial term (eq. 5) in order to improve the performance of COSMO-SAC model. The activity coefficient is expressed by the following equation, referred to as the COSMO-SAC-FV model:

$$ln\,\gamma_{i/s} = ln\,\gamma_{i/s}^{res} + ln\,\gamma_{i/s}^{fv} \tag{26}$$

Where the free volume term $ln\,\gamma_{i/s}^{fv}$ is given by

$$ln\,\gamma_{i/s}^{fv} = ln\frac{\phi_i^{fv}}{x_i} + 1 - \frac{\phi_i^{fv}}{x_i} \tag{27}$$

The ϕ_i^{fv} is the free volume fraction of component *i* and can be expressed as

$$\phi_i^{fv} = \frac{x_i V_{f,i}}{\sum_j x_j V_{f,j}} \tag{28}$$

The free volume of component *i*, $V_{f,i}$, is defined as

$$V_{f,i} = V_i - V_{h,i} \tag{29}$$

Where V_i and $V_{h,i}$ denote the liquid molar volume and the hard core volume of component *i*, respectively.

The liquid molar volume of solvents can be obtained from DIPPR 801 database[55] directly and the hard core volume is assumed to be the van der Waals volume as calculated by the method proposed by Bondi.[56] However, the experimental data for polymers are often unavailable. In such a case, the empirical correlation of Tait[57, 58] and the GCVOL group contribution model[59, 60] are often used. In order to avoid the ambiguity of determining the polymer density, the GCVOL

method is chosen in this work, except for polyethylene, PE. The correlation of Tait allows for discriminating the phase behaviors of LDPE (low density PE) and HDPE (high density PE).

3. Computational details

The σ-profile of each component, a histogram of the screening charge density distribution on the molecular surface, is the most important input for the COSMO-SAC model. The screening charges can be obtained from DFT/COSMO calculations[51] using commercial package DMol3 implemented in Cerius2.[61] The equilibrium molecular geometry is obtained from energy minimization in the ideal gas phase using the density functional theory with nonlocal VWN-BP functional at the DNP v4.0 basis set. A subsequent COSMO calculation is then performed to obtain the molecular surface area, volume, and the screening charges. The σ-profile can be obtained according to eqs. 9 to 13. For homopolymers, the screening charges of a tri-mer are first determined. The σ-profile of corresponding polymer with a desired molecular weight can be obtained by increasing the surface area of the middle unit of the tri-mer after the charge averaging (eq. 9) is done. The degree of polymerization (N_{units}) of the homopolymer can be determined from the molecular weight of polymer ($M_{polymer}$) and monomer ($M_{monomer}$) as $N_{units} = M_{polymer} / M_{monomer}$. For copolymers, the degree of polymerization of monomer A ($N_{units,A}$) and monomer B ($N_{units,B}$) are estimated from the weight fraction of monomer A (r_A) and B (r_B) and the molecular weight of monomer A ($M_{monomer,A}$) and B ($M_{monomer,B}$) as $N_{units,A} = \left(M_{polymer} \cdot \left(r_A / r_A + r_B \right) \right) / M_{monomer,A}$, $N_{units,B} = \left(M_{polymer} \cdot \left(r_B / r_A + r_B \right) \right) / M_{monomer,B}$. The molecular weight of polymers in this work is number average molecular weight Mn (g/mol). If number average molecular weight is not available, the weight average molecular weight Mw

(g/mol) or viscosity average molecular weight Mv (g/mol) would be used instead. For solvents, the freely available VT-database[62, 63] for the COSMO calculation results was used. The pure vapor pressure of solvents in this work are taken from the DIPPR 801 database.[55] To measure the accuracy of the proposed method, we compared the activity of solvent obtained from the experimental data,

$$a^{exp}(T, x_{solvent}) = \frac{P^{exp}(T, x_{solvent})}{P^{vap}_{solvent}(T)} \tag{30}$$

to that obtained from COSMO-SAC calculation ($a^{cal} = x_{solvent}\gamma_{solvent}$)

$$AAD\% = \frac{1}{n}\sum \frac{\left|a^{cal} - a^{exp}\right|}{a^{exp}} \cdot 100\% \tag{31}$$

where n is number of experimental data points.

The solvent activities (*a*) are also plotted against the solvent weight fractions (*w*) and compare to the experimental data. The solvent weight fraction is determined from the following equation:

$$w = \frac{M_{solvent}}{M_{solvent} + M_{polymer}} \tag{32}$$

where $M_{solvent}$ and $M_{polymer}$ denote the weight of solvent and polymer, respectively.

4. Results and discussion

4.1 Vapor-liquid equilibrium of homopolymer solutions

Binary vapor liquid equilibrium systems of 25 homopolymers and 40 solvents with temperatures ranging from 274.15 K to 477.15 K are examined in this work (a complete list of systems considered in this work is provided as Supporting Information). Most of the experimental data are taken from the DECHEMA[64] data bank and other open literature.[64-84] The

overall accuracy in the predicted solvent activity (defined in eq. 33) of all the systems (1377 data points) is 19.2% from the COSMO-SAC model (see Table 1). The replacement of the SG combinatorial term with free volume term developed here, denoted as COSMO-SAC-FV, (eq. 23, 26, and 31) reduces the AAD to 16.4%. The improvement is quite significant for polymer systems such as cis-1,4-PB, cis-1,4-PIP and PVC, while the predictions become less accurate for PE and PVOH. (Note that the full name of the polymers are provided in Table S1 of Supporting Information) The polymers considered in this work not only cover from the simplest polyethylene (PE) to polymers which contain strongly interacting groups within the main polymer chain such as poly (vinyl alcohol) (PVOH).

Also shown in Table 1 are the AAD of COSMO-SAC predictions based on the DFT/COSMO calculations for the monomers (rather than the trimmers). Although the QM calculations are much computationally inexpensive for monomers, the prediction accuracy (AAD=26.5%) is significantly worse. The results indicate that the neighboring units in the tri-mer have strong effects on the screening charges of each monomer. Considering that the prediction results here is similar or more accurate than the previous work of Yang et al.[45] where the σ-profile of the polymer were obtained up to 10-mers, the use of tri-mer could be a good balance between computational cost and prediction accuracy.

Figure 2 illustrates an example of polystyrene (PS) mixed with two solvents of very different polarities, toluene and trichloromethane, respectively. The activity of the solvents is plotted against their weight fractions. The COSMO-SAC prediction is accurate for PS mixed with both solvents. Note that the molecular weights of PS in these two experimental data sets are different but the calculations are done based on the same quantum mechanical result, i.e., a tri-mer of PS.

To further examine the performance of the proposed method on polymers of different molecular weights, Figure 3 illustrates the activity of benzene mixed with PS with molecular weights (Mn) of 800, 20000 and 500000 g/mol, respectively. The experimental data shows that the activity of solvent increases with the molecular weight of the polymer. Furthermore, the solvent activity converges when the molecular weight of the polymer is larger than 20000 g/mol. The COSMO-SAC model predicts not only the difference between the molecular weights but also the convergence of activity at large molecular weights. The method we presented here is also quite accurate for the describing the temperature effects on solvent activity. Figure 4 illustrates the activity of toluene at different temperatures when mixed with PS. The decrease of toluene activity with increasing temperature is correctly predicted by the COSMO-SAC model.

Also provide in Figures 2 to 4 are the predictions from COSMO-SAC-FV. It can be seen that the solvent activity predictions are slightly increased with the effect of free volume taken into account. However, in some systems such as the mixture of cis-1,4-PIP with p-xylene and the mixture of PVC with tetrahydrofuran as shown in Figure 5, the free volume term will largely enhance the solvent activity and lead to a better prediction.

Table 2 compares the performance of the COSMO-SAC model to those from other predictive activity coefficient models, including UNIFAC-FV,[32] Entropic-FV[35] and UNIFAC-ZM.[41] The AAD% of these models are taken from the literature.[32, 85] (complete list of the systems is provided as Supporting Information) Although the overall AAD from COSMO-SAC (9.3%) and COSMO-SAC-FV (7.4%) is higher than that from UNIFAC-FV (5.8%), COSMO-SAC is in fact comparable to UNIFAC-FV in most cases except for PH/toluene and PS/ketone systems. It should be pointed out that there are two parameters of free volume term in UNIFAC-FV were optimized for polymer solutions, whereas the COSMO-SAC model was not (all the

model parameters are taken from the literature[49]). From Table 2 it can be seen that the prediction of COSMO-SAC-FV (11.4%) model is comparable to the results of Entropic-FV (10.8%) and UNIFAC-ZM (13.8%) (489 data points). The slightly higher error of COSMO-SAC-FV can be attributed to the large number of PIB and alkane mixtures. The COSMO-SAC-FV model proposed here can accurately predict the VLE of polymer solutions. When the density information is unavailable, the COSMO-SAC itself can provide satisfactory predictions. The predictive power of COSMO-SAC and COSMO-SAC-FV models for systems not used in parameterization makes it an useful method when FV-based UNIFAC model is not applicable (e.g., due to missing parameters and density information of polymers).

It is noteworthy that some of the polymers may be in one of the possible tacticities: isotactic, syndiotactic, or atatic. Unfortunately, the tacticity of the polymeric materials used in the VLE measurements are not always specified. Nonetheless, the proposed method is capable of distinguishing the VLE of the same polymer in different tacticities. In Table 3, we report the accuracy of COSMO-SAC based on isotatic and syndiotactic configurations of several polymers. In most cases, the same polymer with a different tacticity shows a similar VLE behavior. However, in some cases, the difference can be significant. For example, the overall deviation is 25.6% for isotactic PVME but only 6.5% for syndiotactic PVME. From Figure 6, different results can be seen when trichloromethane mixed with isotactic PVME and syndiotactic PVME, respectively. Since the polymer tacticity were unknown for most of the reported VLE data, the deviations of such systems are averaged from isotactic and syndiotactic polymers. Our result indicates that polymer tacticity may indeed affect its VLE and the COSMO-SAC model can be used to study such effects.

4.2 Vapor-liquid equilibrium of copolymer solutions

Eight copolymers and 22 solvents with temperatures ranging from 298.15 K to 423.15 K are examined in this work. The experimental data of copolymer mixture are mainly from CRC handbook and other literatures.[64, 86-88] The overall accuracy in the predicted solvent activity of all copolymer systems (872 data points) is 12.7% from the COSMO-SAC model and 13.0% from COSMO-SAC-FV model. From Table 4 it can be seen that the use of tetra-mer configuration of A-A-B-B results in about 4% reduction in the AAD compared to that based on A-B-A-B configurations. Di-block and tri-block copolymer systems are also accurately predicted by COSMO-SAC and COSMO-SAC-FV models with the arrangement of A-A-B-B since the VLE data of block and random copolymer solutions show little difference. The prediction accuracy from COSMO-SAC models are comparable to other group contribution methods (9.5% from Entropic-FV and 9.4% from UNIFAC-ZM) as shown in Table 2.

Figure 7(a) illustrates the activity of trichloromethane in homopolymers PMMA and PS homopolymers, and the copolymer S-MMA/50w. The COSMO-SAC-FV model correctly predicts that the trichloromethane activity in S-MMA/50w lies between that in PMMA and PS, as observed in experiments. Figure 7(b) illustrates an interesting case where the solvent (toluene) activity in copolymer (VA-E/41.8w) solution falls below both homopolymers (PVA and PE). Such behavior has been attributed to the steric hindrance of the repeating units of PVA, which restrains the interactions between toluene and acetate group and makes toluene less dissolvable in PVA solution.[89] Interestingly the COSMO-SAC-FV model can successfully describe this special behavior.

4.3 Liquid-liquid equilibrium of polymer solutions

COSMO-SAC and COSMO-SAC-FV models are applied to the liquid-liquid equilibrium prediction for 13 polymer solutions shown in Table 5. It can be seen that COSMO-SAC-FV model can describe various LLE phase behaviors including upper critical solution temperature (UCST), lower critical solution temperature (LCST), closed loop and hourglass phase behaviors while COSMO-SAC model often misses LCST and hourglass behaviors. The more pronounced free-volume effects near the critical region could be the reason for the failure of COSMO-SAC in predicting the LCST of polymer solutions. Although both of the models fail to describe the phase separation in some polymer solutions, the COSMO-SAC-FV model does describe some polymer systems with qualitative agreement with experiments and is comparable to the group contribution methods including Entropic-FV, GC-Flory EOS and GC-LF EOS model. So far there is no purely predictive group contribution model that can accurately describe both VLE and LLE phase behavior of polymer solutions without re-parameterization or input of some experimental data.[44] From Figure 8, it can be seen that COSMO-SAC-FV model successfully predicts the UCST of cyclohexane in PS and both UCST and LCST in PαMS (the experimental data taken from the literature[90]). The change of immiscibility gap with molecular weight of polymer (Fig. 8(a)) is successfully predicted. Furthermore, the tacticity has a significant effect on the phase boundary (Fig. 8(a)). The coexistence curves of syndiotactic PS mixture are higher than the curves of isotactic PS mixture. This again shows that the COSMO-SAC model can be used to study the effect of tacticity in the phase behavior of polymer solutions.

5. Conclusions

The COSMO-SAC model is studied for its predictive power in describing the phase behaviors of polymer solutions. The main challenge here is the proper representation of polymers

with the time-consuming quantum mechanical calculations. By assuming that the screening charges are not much affected by intra-molecular long range interactions, we propose a method to generate the surface charge distribution (or the σ-profile) of polymers using the DFT/COSMO calculation of tri-mers for homopolymers and tetra-mers for copolymers. Without any further modification and parameter fitting, the COSMO-SAC model provides the prediction of solvent activity comparable to group contribution methods. The free volume effects, known to be important in polymer solutions, can be incorporated into the COSMO-SAC model, the COSMO-SAC-FV model. The replacement of the SG term with the free volume model of Elbro improves the prediction accuracy both for VLE and LLE. The COSMO-SAC model also successfully predicts the change of solvent activity with the molecular weight, system temperatures, tacticity of a polymer and detailed intra-molecular effect in copolymer mixtures. Therefore the COSMO-SAC model can be used to study the subtle molecular structure and conformation effects on the phase behavior of polymer solutions. The inclusion of different polymer chain configurations in the COSMO-SAC model may be a way for more accurate prediction of polymer phase behaviors.

Acknowledgements

This research was partially supported by the National Science Council of Taiwan (NSC 101-2628-E-002-014-MY3 and 102-3113-P-002-010) and Ministry of Education of Taiwan (101R70815 and 102R7815). The computation resources from the National Center for High-Performance Computing of Taiwan and the Computing and Information Networking Center of the National Taiwan University are acknowledged.

Supporting Information Available

A complete list of systems considered in this work is provided as Supporting Information . This information is available free of charge via the Internet at http://pubs.acs.org/.

References

(1) McKenna, T. F.; Malone, M. F. Polymer process design .1. Continuous production of chain growth homopolymers. *Comput. Chem. Eng.* **1990,** *14*, 1127-1149.

(2) Pfohl, O.; Dohrn, R. Provision of thermodynamic properties of polymer systems for industrial applications. *Fluid Phase Equilib.* **2004,** *217*, 189-199.

(3) Stephan, W.; Noble, R. D.; Koval, C. A. Design methodology for a membrane distillation column hybrid process. *J. Membr. Sci.* **1995,** *99*, 259-272.

(4) Bogdanic, G.; Fredenslund, A. Revision of the group-contribution flory equation of state for phase-equilibria calculations in mixtures with polymers .1. Prediction of vapor-liquid-equilibria for polymer-solutions. *Ind. Eng. Chem. Res.* **1994,** *33*, 1331-1340.

(5) Chen, F.; Fredenslund, A.; Rasmussen, P. Group-contribution flory equation of state for vapor-liquid equilibria in mixtures with polymers. *Ind. Eng. Chem. Res.* **1990,** *29*, 875-882.

(6) High, M. S.; Danner, R. P. A group contribution equation of state for polymer-solutions. *Fluid Phase Equilib.* **1989,** *53*, 323-330.

(7) High, M. S.; Danner, R. P. Application of the group contribution lattice-fluid eos to polymer solutions. *AIChE J.* **1990,** *36*, 1625-1632.

(8) Holten-Andersen, J.; Rasmussen, P.; Fredenslund, A. Phase equilibria of polymer solutions by group contribution. 1. Vapor-liquid equilibria. *Ind. Eng. Chem. Res.* **1987,** *26*, 1382-1390.

(9) Jones, A. T.; Derawi, S.; Danner, R. P.; Duda, J. L. A simplified approach to vapor-liquid equilibria calculations with the group-contribution lattice-fluid equation of state. *Fluid Phase Equilib.* **2007,** *259*, 116-122.

(10) Lee, S. S.; Sun, Y. K.; Bae, Y. C. Vapor-liquid equilibria for polymer solutions through a group-contribution method: Chain-length dependence. *J. Appl. Polym. Sci.* **2008,** *110*, 2634-2640.

(11) Li, J.; Lei, Z.; Chen, B.; Li, C. Extension of the group-contribution lattice-fluid equation of state. *Fluid Phase Equilib.* **2007,** *260*, 135-145.

(12) Lee, B. C.; Danner, R. P. Group-contribution lattice-fluid eos: Prediction of lle in polymer solutions. *AIChE J.* **1996,** *42*, 3223-3230.

(13) Saraiva, A.; Bogdanic, G.; Fredenslund, A. Revision of the group-contribution flory equation of state for phase-equilibria calculations in mixtures with polymers .2. Prediction of liquid-liquid equilibria for polymer-solutions. *Ind. Eng. Chem. Res.* **1995,** *34*, 1835-1841.

(14) Dominik, A.; Jain, S.; Chapman, W. G. New equation of state for polymer solutions based on the statistical associating fluid theory (saft)-dimer equation for hard-chain molecules. *Ind. Eng. Chem. Res.* **2007,** *46*, 5766-5774.

(15) Gross, J.; Sadowski, G. Perturbed-chain saft: An equation of state based on a perturbation theory for chain molecules. *Ind. Eng. Chem. Res.* **2001,** *40*, 1244-1260.

(16) Pedrosa, N.; Vega, L. F.; Coutinho, J. A. P.; Marrucho, I. M. Phase equilibria calculations of polyethylene solutions from saft-type equations of state. *Macromolecules* **2006,** *39*, 4240-4246.

(17) Sako, T.; Wu, A. H.; Prausnitz, J. M. A cubic equation of state for high-pressure phase equilibria of mixtures containing polymers and volatile fluids. *J. Appl. Polym. Sci.* **1989,** *38*, 1839-1858.

(18) Orbey, N.; Sandler, S. I. Vapor-liquid equilibrium of polymer solutions using a cubic equation of state. *AIChE J.* **1994,** *40*, 1203-1209.

(19) Sanchez, I. C.; Cho, J. A universal equation of state for polymer liquids. *Polymer* **1995,** *36*, 2929-2939.

(20) Bertucco, A.; Mio, C. Prediction of vapor-liquid equilibrium for polymer solutions by a group-contribution redlich-kwong-soave equation of state. *Fluid Phase Equilib.* **1996,** *117*, 18-25.

(21) Zhong, C. L.; Masuoka, H. A new mixing rule for cubic equations of state and its application to vapor-liquid equilibria of polymer solutions. *Fluid Phase Equilib.* **1996,** *123*, 59-69.

(22) Louli, V.; Tassios, D. Vapor-liquid equilibrium in polymer-solvent systems with a cubic equation of state. *Fluid Phase Equilib.* **2000,** *168*, 165-182.

(23) Haghtalab, A.; Espanani, R. A new model and extension of wong-sandler mixing rule for prediction of (vapour plus liquid) equilibrium of polymer solutions using eos/g(e). *J. Chem. Thermodyn.* **2004,** *36*, 901-910.

(24) Voutsas, E.; Magoulas, K.; Tassios, D. Universal mixing rule for cubic equations of state applicable to symmetric and asymmetric systems: Results with the peng-robinson equation of state. *Ind. Eng. Chem. Res.* **2004,** *43*, 6238-6246.

(25) Voutsas, E.; Louli, V.; Boukouvalas, C.; Magoulas, K.; Tassios, D. Thermodynamic property calculations with the universal mixing rule for eos/g(e) models: Results with the peng-robinson eos and a unifac model. *Fluid Phase Equilib.* **2006,** *241*, 216-228.

(26) Wang, L. S. Calculation of vapor-liquid equilibria of polymer solutions and gas solubilities in molten polymers based on psrk equation of state. *Fluid Phase Equilib.* **2007,** *260*, 105-112.

(27) Staudt, P. B.; Soares, R. d. P.; Secchi, A. R.; Cardozo, N. S. M. A new cubic equation of state for prediction of vle of polymer solutions. *Fluid Phase Equilib.* **2010,** *295*, 38-45.

(28) Baniasadi, M.; Ghader, S. Description of polymer solutions phase equilibria by cubic equation of state with different mixing rules. *J. Eng. Thermophys.* **2011,** *20*, 115-127.

(29) Flory, P. J. *Principles of polymer chemistry*. Cornell University Press: Ithaca, 1953.

(30) Huggins, M. L. *Physical chemistry of high polymers,*. Willey: New York, 1958.

(31) Bae, Y. C.; Shim, J. J.; Soane, D. S.; Prausnitz, J. M. Representation of vapor liquid and liquid liquid equilibria for binary-systems containing polymers - applicability of an extended flory huggins equation. *J. Appl. Polym. Sci.* **1993,** *47*, 1193-1206.

(32) Oishi, T.; Prausnitz, J. M. Estimation of solvent activities in polymer solutions using a group-contribution method. *Ind. Eng. Chem. Proc. Des. Dev.* **1978,** *17*, 333-339.

(33) Patterso.D Free volume and polymer solubility . A qualitative view. *Macromolecules* **1969,** *2*, 672-677.

(34) Flory, P. J. Thermodynamics of polymer solutions. *Discuss. Faraday Soc.* **1970**, 7-29.

(35) Kontogeorgis, G. M.; Fredenslund, A.; Tassios, D. P. Simple activity coefficient model for the prediction of solvent activities in polymer solutions. *Ind. Eng. Chem. Res.* **1993,** *32*, 362-372.

(36) Elbro, H. S.; Fredenslund, A.; Rasmussen, P. A new simple equation for the prediction of solvent activities in polymer solutions. *Macromolecules* **1990,** *23*, 4707-4714.

(37) Kannan, D. C.; Duda, J. L.; Danner, R. P. A free-volume term based on the van der waals partition function for the unifac model. *Fluid Phase Equilib.* **2005,** *228*, 321-328.

(38) Kouskoumvekaki, I. A.; Michelsen, M. L.; Kontogeorgis, G. M. An improved entropic expression for polymer solutions. *Fluid Phase Equilib.* **2002,** *202*, 325-335.

(39) Liu, Q. L.; Cheng, Z. F. A modified unifac model for the prediction of phase equilibrium for polymer solutions. *J. Polym. Sci., Part B: Polym. Phys.* **2005,** *43*, 2541-2547.

(40) Wibawa, G.; Takishima, S.; Sato, Y.; Masuoka, H. An improved prediction result of entropic-fv model for vapor–liquid equilibria of solvent–polymer systems. *J. Appl. Polym. Sci.* **2005,** *97*, 1145-1153.

(41) Zhong, C. L.; Sato, Y.; Masuoka, H.; Chen, X. N. Improvement of predictive accuracy of the unifac model for vapor-liquid equilibria of polymer solutions. *Fluid Phase Equilib.* **1996,** *123*, 97-106.

(42) Costa, G. M. N.; Dias, T.; Cardoso, M.; Guerrieri, Y.; Pessoa, F. L. P.; de Melo, S. A. B. V.; Embirucu, M. Prediction of vapor-liquid and liquid-liquid equilibria for polymer systems: Comparison of activity coefficient models. *Fluid Phase Equilib.* **2008,** *267*, 140-149.

(43) Kontogeorgis, G. M.; Saraiva, A.; Fredenslund, A.; Tassios, D. P. Prediction of liquid-liquid equilibrium for binary polymer-solutions with simple activity-coefficient models. *Ind. Eng. Chem. Res.* **1995,** *34*, 1823-1834.

(44) Bogdanic, G. Group contribution methods for estimating the properties of polymer systems. *Hemijska industrija* **2006,** *60*, 287-305.

(45) Yang, L.; Xu, X.; Peng, C.; Liu, H.; Hu, Y. Prediction of vapor-liquid equilibrium for polymer solutions based on the cosmo-sac model. *AIChE J.* **2010,** *56*, 2687-2698.

(46) Lin, S. T.; Sandler, S. I. Infinite dilution activity coefficients from ab initio solvation calculations. *AIChE J.* **1999,** *45*, 2606-2618.

(47) Lin, S. T.; Sandler, S. I. Prediction of octanol-water partition coefficients using a group contribution solvation model. *Ind. Eng. Chem. Res.* **1999,** *38*, 4081-4091.

(48) Lin, S. T.; Sandler, S. I. A priori phase equilibrium prediction from a segment contribution solvation model. *Ind. Eng. Chem. Res.* **2002,** *41*, 899-913.

(49) Hsieh, C.-M.; Sandler, S. I.; Lin, S.-T. Improvements of cosmo-sac for vapor-liquid and liquid-liquid equilibrium predictions. *Fluid Phase Equilib.* **2010,** *297*, 90-97.

(50) Staverman, A. J. The entropy of high polymer solutions. Generalization of formulae. *Recl. Trav. Chim. Pays-Bas-J. Roy. Neth. Chem. Soc.* **1950,** *69*, 163-174.

(51) Klamt, A.; Schuurmann, G. Cosmo: A new approach to dielectric screening in solvents with explicit expressions for the screening energy and its gradient. *J. Chem. Soc., Perkin Trans. 2* **1993**, 799-805.

(52) Lin, S. T.; Chang, J.; Wang, S.; Goddard, W. A.; Sandler, S. I. Prediction of vapor pressures and enthalpies of vaporization using a cosmo solvation model. *J. Phys. Chem. A* **2004,** *108*, 7429-7439.

(53) Lin, S. T.; Sandler, S. I. A priori phase equilibrium prediction from a segment contribution solvation model. *Ind. Eng. Chem. Res.* **2004,** *43*, 1322-1322.

(54) Wang, S.; Sandler, S. I.; Chen, C.-C. Refinement of cosmo-sac and the applications. *Ind. Eng. Chem. Res.* **2007,** *46*, 7275-7288.

(55) Project 801, evaluated process design data, public release documentation, design institute for physical properties (dippr), american institute of chemical engineers (aiche)

In 2006.

(56) Bondi, A. A. *Physical properties of molecular crystals, liquids and glasses*. John Wiley & Sons: New York, 1968.

(57) Tait, P. G. *Physics and chemistry of the voyage of h.M.S. Challenger*. HMSO: London, 1888; Vol. 2.

(58) Rodgers, P. A. Pressure volume temperature relationships for polymeric liquids - a review of equations of state and their characteristic parameters for 56 polymers. *J. Appl. Polym. Sci.* **1993,** *48*, 1061-1080.

(59) Elbro, H. S.; Fredenslund, A.; Rasmussen, P. Group contribution method for the prediction of liquid densities as a function of temperature for solvents, oligomers, and polymers. *Ind. Eng. Chem. Res.* **1991,** *30*, 2576-2582.

(60) Ihmels, E. C.; Gmehling, J. Extension and revision of the group contribution method gcvol for the prediction of pure compound liquid densities. *Ind. Eng. Chem. Res.* **2003,** *42*, 408-412.

(61) *Cerius2, dmol3, version 4.0*, Molecular Simulations Inc: San Diego, CA 1999.

(62) Mullins, E.; Liu, Y. A.; Ghaderi, A.; Fast, S. D. Sigma profile database for predicting solid solubility in pure and mixed solvent mixtures for organic pharmacological compounds with cosmo-based thermodynamic methods. *Ind. Eng. Chem. Res.* **2008,** *47*, 1707-1725.

(63) Mullins, E.; Oldland, R.; Liu, Y. A.; Wang, S.; Sandler, S. I.; Chen, C. C.; Zwolak, M.; Seavey, K. C. Sigma-profile database for using cosmo-based thermodynamic methods. *Ind. Eng. Chem. Res.* **2006,** *45*, 4389-4415.

(64) Wen H, E. H., Alessi P *Polymer solution data collection*. DECHEMA: *Frankfurt*, 1992.

(65) Bawn, C. E. H.; Freeman, R. F. J.; Kamaliddin, A. R. High polymer solutions part 1.- vapour pressure of polystyrene solutions. *Trans. Faraday Soc.* **1950,** *46*, 677-684.

(66) Bawn, C. E. H.; Wajid, M. A. High polymer solutions part 7.- vapour pressure of polystyrene solutions in acetone, chloroform and propyl acetate. *Trans. Faraday Soc.* **1956,** *52*, 1658-1664.

(67) McGlashan, M.; Williamson, A. G. Thermodynamics of mixtures of n-hexane+n-hexadecane. Part 2.- vapour pressures and activity coefficients. *Trans. Faraday Soc.* **1961,** *57*, 588-600.

(68) Eichinge.Be; Flory, P. J. Thermodynamics of polymer solutions part 2.-polyisobutylene and benzene. *Trans. Faraday Soc.* **1968,** *64*, 2053-2060.

(69) Eichinge.Be; Flory, P. J. Thermodynamics of polymer solutions part 3.-polyisobutylene and cyclohexane. *Trans. Faraday Soc.* **1968,** *64*, 2061-2065.

(70) Eichinge.Be; Flory, P. J. Thermodynamics of polymer solutions part 4.-polyisobutylene and n-pentane. *Trans. Faraday Soc.* **1968,** *64*, 2066-2072.

(71) Tait, P. J. T.; Livesey, P. J. Thermodynamic studies on poly(alpha-olefin)-solvent systems. *Polymer* **1970,** *11*, 359-373.

(72) Booth, C.; Devoy, C. J. Thermodynamics of mixtures off poly(ethylene oxide) and benzene. *Polymer* **1971,** *12*, 309-319.

(73) Booth, C.; Devoy, C. J. Thermodynamics of mixtures of poly(propylene oxide) and benzene. *Polymer* **1971,** *12*, 320-326.

(74) Brockmei.Nf; McCoy, R. W.; Meyer, J. A. Gas-chromatographic determination of thermodynamic properties of polymer-solutions .2. Semicrystalline polymer systems. *Macromolecules* **1973,** *6*, 176-180.

(75) Bonner, D. C.; Brockmei.Nf; Cheng, Y. L. Thermodynamics of some concentrated high polymer-solutions. *Ind. Eng. Chem. Proc. Des. Dev.* **1974,** *13*, 437-441.

(76) Matsumura, K.; Katayama, T. Vapor liquid equilibria of binary dand ternary solutions containing polyvinyl acetate as a component. *Kagaku Kogaku* **1974,** *38*, 388-392.

(77) Wang, N. H.; Takishima, S.; Masuoka, H. Solubility of benzene, toluene and cyclohexane in polystyrene below its glass-transition temperature. *Kag. Kog. Ronbunshu* **1989,** *15*, 795-803.

(78) Gupta, R. B.; Prausnitz, J. M. Vapor-liquid equilibria of copolymer + solvent and homopolymer + solvent binaries: New experimental data and their correlation. *J. Chem. Eng. Data* **1995,** *40*, 784-791.

(79) Tanbonliong, J. O.; Prausnitz, J. M. Vapour-liquid equilibria for some binary and ternary polymer solutions. *Polymer* **1997,** *38*, 5775-5783.

(80) Kim, J.; Joung, K. C.; Hwang, S.; Huh, W.; Lee, C. S.; Yoo, K. P. Measurement of vapor sorption equilibria of polymer solutions and comparative correlation by g(e)-models and lattice equations of state. *Korean J. Chem. Eng.* **1998,** *15*, 199-210.

(81) Jung, J. K.; Joung, S. N.; Shin, H. Y.; Kim, S. Y.; Yoo, K. P.; Huh, W.; Lee, C. S. Measurements and correlation of hydrogen-bonding vapor sorption equilibrium data of binary polymer solutions. *Korean J. Chem. Eng.* **2002,** *19*, 296-300.

(82) Palamara, J. E.; Zielinski, J. M.; Hamedi, M.; Duda, J. L.; Danner, R. P. Vapor-liquid equilibria of water, methanol, and methyl acetate in poly(vinyl acetate) and partially and fully hydrolyzed poly(vinyl alcohol). *Macromolecules* **2004,** *37*, 6189-6196.

(83) Wohlfarth, C. *Crc handbook of thermodynamic data of aqueous polymer solutions*. CRC Press: Boca Raton, FL, 2004.

(84) Wohlfarth, C. *Landolt-börnstein: Numerical data and functional relationships in science and technology - new series, part 6d1*. Springer: 2009.

(85) Pappa, G. D.; Voutsas, E. C.; Tassios, D. P. Prediction of activity coefficients in polymer and copolymer solutions using simple activity coefficient models. *Ind. Eng. Chem. Res.* **1999,** *38*, 4975-4984.

(86) Wohlfarth, C. *Crc handbook of thermodynamic data of copolymer solutions*. CRC Press: Boca Raton, 2001.

(87) Kang, S. H.; Huang, Y. M.; Fu, J. Y.; Liu, H. L.; Hu, Y. Vapor-liquid equilibria of several copolymer plus solvent systems. *J. Chem. Eng. Data* **2002,** *47*, 788-791.

(88) Se, R. A. G.; Aznar, M. Vapor-liquid equilibrium of copolymer plus solvent systems: Experimental data and thermodynamic modeling with new unifac groups. *Chin. J. Chem. Eng.* **2008,** *16*, 605-611.

(89) Jones, A. T.; Zielinski, J. M.; Danner, R. P. Solubility predictions for copolymer systems. *Fluid Phase Equilib.* **2009,** *280*, 88-93.

(90) Wohlfarth, C. *Crc handbook of liquid-liquid equilibrium data of polymer solutions*. CRC Press: Boca Raton, FL, 2007.

Tables

Table 1. Comparison of prediction accuracy (AAD%) of solvent activity in homopolymer solutions from COSMO-SAC models

polymer	solvents[a]	data[b]	COSMO-SAC		COSMO-SAC-FV
			tri-mer[c]	monomer[c]	tri-mer
PE	7	67	16.8	16.5	25.8
PH	1	21	16.2	7.1	12.3
cis-1,4-PB	7	45	21.8	25.1	16.2
PP	3	37	19.6	21.3	16.9
PIB	12	287	15.5	26.9	14.8
PS	12	266	9.4	19.5	8.6
PαMS	2	17	2.8	11.4	3.7
PVK	1	22	23.2	22.4	-[d]
cis-1,4-PIP	5	44	32.7	36.1	13.1
PDMS	7	117	23.7	38.5	-[d]
PEO	3	78	35.9	27.4	20.5
PEG	1	6	13.2	49.9	4.4
PPO	2	41	15.3	18.6	12.1
PEGDE	2	17	48.8	20.8	51.2
PPGDE	2	24	40.1	20.4	36.6
PVME	2	26	16.1	16.0	13.4
PVC	5	44	28.3	47.2	15.1
PMA	2	12	11.5	26.6	5.5
PMMA	6	47	9.5	22.7	8.7
PEA	2	12	5	17.6	4.6

PEMA	2	11	5.9	15.2	3.2
PBA	2	12	3.7	10.4	9.7
PVA	8	93	22.9	29.8	18.3
PAN	2	23	53.3	90.0	39.7
PVOH	2	8	26.6	38.1	68.7
overall	40	1377	19.2	26.5	16.4

[a]: number of solvents

[b]: number of data points

[c]: The σ-profile of polymer is generated based on a monomer unit or a tri-mer

[d]: Volume information is unavailable for free volume estimation.

Table 2. Comparison of prediction accuracy (AAD%) of solvent activity in homopolymer solutions various activity coefficient models

polymer	n	AAD%				
		COSMO-SAC	COSMO-SAC-FV	UNIFAC-FV[32]	Entropic-FV[35]	UNIFAC-ZM[41]
homopolymer	1377	19.2	16.4[a]	-	-	-
homopolymer	489	14.8	11.4	-	10.8	13.8
homopolymer	234	9.3	7.4	5.8	-	-
copolymer	872	12.7	13.2	-	-	-
copolymer	155	12.0	11.1	-	9.5	9.4

[a] : Staverman-Guggenheim combinatorial term is used when the volume information for the free volume term is missing

Table 3. Comparison of prediction accuracy (AAD%) of solvent activity in homopolymer solutions from COSMO-SAC using isotactic and syndiotactic polymer structures

polymer	#solvent	temperature range (K)	n	polymer structures	
				isotactic	syndiotactic
PP	3	298.15	37	18.3	20.9
PS	12	293.15-353.15	266	8.7	10.0
PVME	5	298.15	26	25.6	6.5
PVC	2	315.65-338.15	44	26.1	30.5
PVA	8	303.15~353.15	93	21.0	24.9
PAN	2	333.15-353.15	23	37.9	68.8
PVOH	2	303.15-383.15	8	23.6	29.6
overall	21	293.15-383	497	15.7	18.3

Table 4. Comparison of prediction accuracy (AAD%) of solvent activity in copolymer solutions from COSMO-SAC

copolymer	weight fraction range (monomer A) (%)	temperature range (K)	n	COSMO-SAC		COSMO-SAC-FV	
				AABB[a]	ABAB[b]	AABB[a]	ABAB[b]
S-MMA	41.45-50	298.15-398.15	134	9.8	9.8	10.0	9.9
S-BR	4.1-45	308.15-403.15	204	10.1	11.4	12.6	12.7
S-AN	70-75	313.15-423.15	103	7.5	8.2	9.8	5.5
S-BMA	50	333.15-343.15	21	29.3	32.2	27.9	28.0
VA-E	3.6-70	303.15-383.15	277	11.9	25.7	10.5	26.1
VA-VC	10-12	353.15-398.15	48	52.1	54.4	56.3	60.3
EO-PO	7-53	303.15-343.15	54	8.6	7.1	7.6	6.5
VAL-VA	70-96.6	298.15	31	0.1	0.02	0.1	0.04
overall	3.6-96.6	298.15-423.15	872	12.7	17.5	13.2	17.8

[a]: The tetra-mer used in the DFT/COSMO calculation is arranged as A-A-B-B

[b]: The tetra-mer used in the DFT/COSMO calculation is arranged as A-B-A-B

Table 5. Comparison of Predicted Liquid-Liquid Equilibria from COSMO-SAC Models with Experimental Data

polymer	solvent	COSMO-SAC	COSMO-SAC-FV	exp[a]
PS	cyclohexane	UCST	UCST	UCST, LCST
PαMS	cyclohexane	UCST	UCST, LCST	UCST, LCST
PEO	methanol	no phase separation	LCST	LCST
PS	methyl acetate	UCST	UCST, LCST	UCST, LCST
PIB	benzene	UCST	UCST, LCST	UCST, LCST
PVOH	water	closed loop	closed loop	closed loop
HDPE	1-octanol	UCST	hourglass	UCST
PB	1-octane	only UCST	only UCST	hourglass, LCST, UCST
PEG	water	UCST	LCST	closed loop
PEG	tert-butyl acetate	no phase separation	no phase separation	hourglass, LCST, UCST
PMMA	4-heptanone	no phase separation	no phase separation	UCST
PS	acetone	no phase separation	no phase separation	hourglass, LCST, UCST
PIB	hexane	no phase separation	no phase separation	hourglass, LCST, UCST

[a]: experimental coexistence curve

Figure captions

Figure 1. (a) the σ-profile of a PVOH tri-mer (b) the σ-profile of the middle monomer in a PVOH tri-mer (c) the σ-profile of polymer PVOH (Mn=14700 g/mol).

Figure 2. The activity of toluene (circles) in its mixture with polymer PS (Mn=154000 g/mol) and activity of trichloromethane (squares) in its mixture with polymer PS (Mn=90000 g/mol) at 298.15K from experiment[64] (open symbols), COSMO-SAC prediction (solid line for toluene and dotted line for trichloromethane) and COSMO-SAC-FV prediction (dash line).

Figure 3. The activity of benzene (circles) in its mixture with polymer PS (Mn=800 g/mol) at 298.15K, (squares) with polymer PS (Mn=20000 g/mol) at 293.15K and (triangles) with polymer PS (Mn=500000 g/mol) at 293.15K from experiment[64] (open symbols), COSMO-SAC prediction (solid line for polymer PS (Mn=800 g/mol), dotted line for polymer PS (Mn=20000 g/mol), dash line for polymer PS (Mn=500000 g/mol)) and COSMO-SAC-FV (red long dash line).

Figure 4. The activity of toluene at different temperatures (T) when mixed with polymer PS (Mn=290000 g/mol) at similar solvent weight fractions (*w*) from experiment[64] (open circles), COSMO-SAC prediction (solid line) and COSMO-SAC-FV prediction (dash line).

Figure 5. (a) The activity of p-xylene (circles) in its mixture with polymer cis-1,4-PIP (Mn=800000 g/mol) at 293.2K from experiment[84] (open symbols), COSMO-SAC prediction (solid line) and COSMO-SAC-FV prediction (dash line). (b) The activity of tetrahydrofuran (circles) in its mixture with polymer PVC (Mn=34000 g/mol) at 293.2K from experiment[64] (open symbols), COSMO-SAC prediction (solid line) and COSMO-SAC-FV prediction (dash line).

Figure 6. The activity of trichloromethane in its mixture with polymer PVME (Mn=14000 g/mol) at 298.15K from experiment[64] (open circles), COSMO-SAC predictions based on syndiotactic (solid line) and isotactic (dotted line) configurations and COSMO-SAC-FV prediction (dash line). The molecular structures of tri-mer are shown next to the corresponding curves.

Figure 7. (a) The UCST behavior of cyclohexane in its mixture with polymer PS in different tacticity, PS (Mn=19200 g/mol) (circles), PS (Mn=34900 g/mol) (triangles) and PS (Mn=94300 g/mol) (squares) from experiment (open symbols)[90]; COSMO-SAC-FV predictions (solid line for polymer PS (Mn=19200 g/mol), dotted line for polymer PS (Mn=34900 g/mol), dash line for polymer PS (Mn=94300 g/mol)) (b) The UCST and LCST behaviors of cyclohexane in its mixture with polymer PaMS (Mn=289200 g/mol) from experiment (circles)[90] and COSMO-SAC-FV prediction (solid lines)

Figure 8. (a) The UCST behavior of cyclohexane in its mixture with polymer PS in different tacticity, PS (Mn=19200 g/mol) (circles), PS (Mn=34900 g/mol) (triangles) and PS (Mn=94300 g/mol) (squares) from experiment (open symbols)[90]; COSMO-SAC-FV predictions (solid line for polymer PS (Mn=19200 g/mol), dotted line for polymer PS (Mn=34900 g/mol), dash line for polymer PS (Mn=94300 g/mol)) (b) The UCST and LCST behaviors of cyclohexane in its mixture with polymer PaMS (Mn=289200 g/mol) from experiment (circles)[90] and COSMO-SAC-FV prediction (solid lines)

Figures

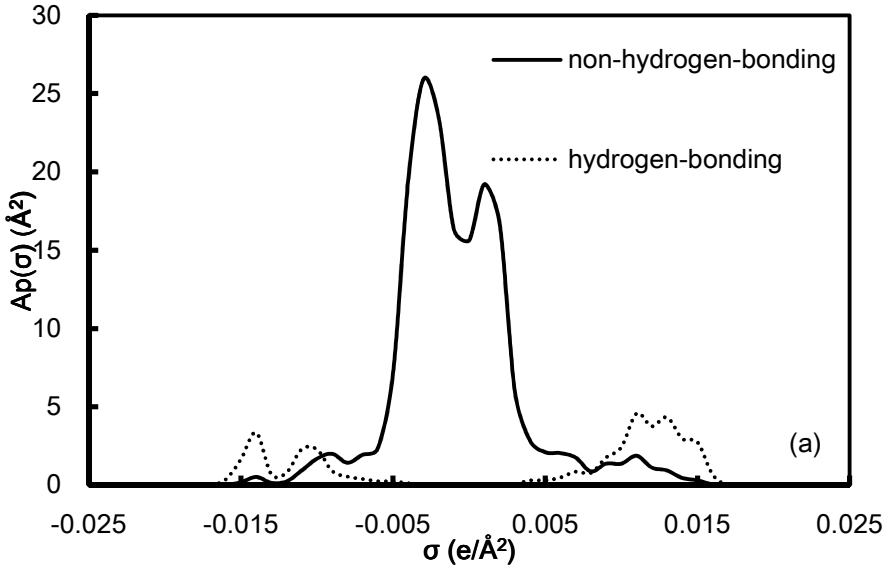
non-hydrogen-bonding
hydrogen-bonding
Ap(σ) (Å²)
σ (e/Å²)
(a)

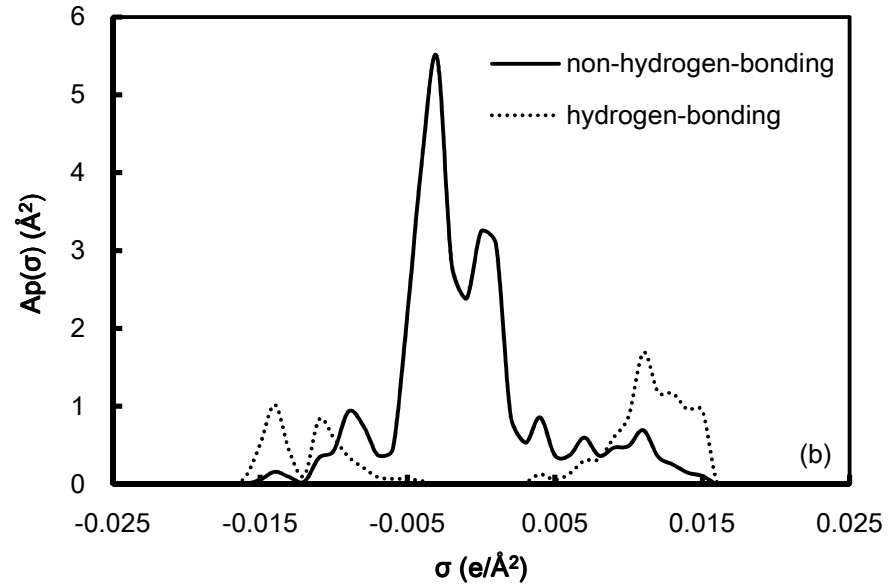
non-hydrogen-bonding
hydrogen-bonding
Ap(σ) (Å²)
σ (e/Å²)
(b)

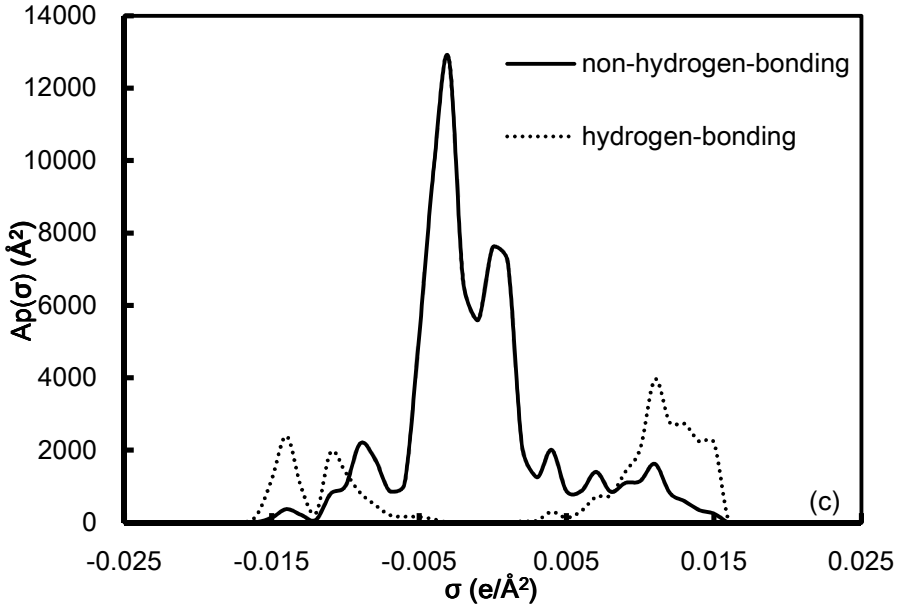

Figure 1. (a) the σ-profile of a PVOH tri-mer (b) the σ-profile of the middle monomer in a PVOH tri-mer (c) the σ-profile of polymer PVOH (Mn=14700 g/mol).

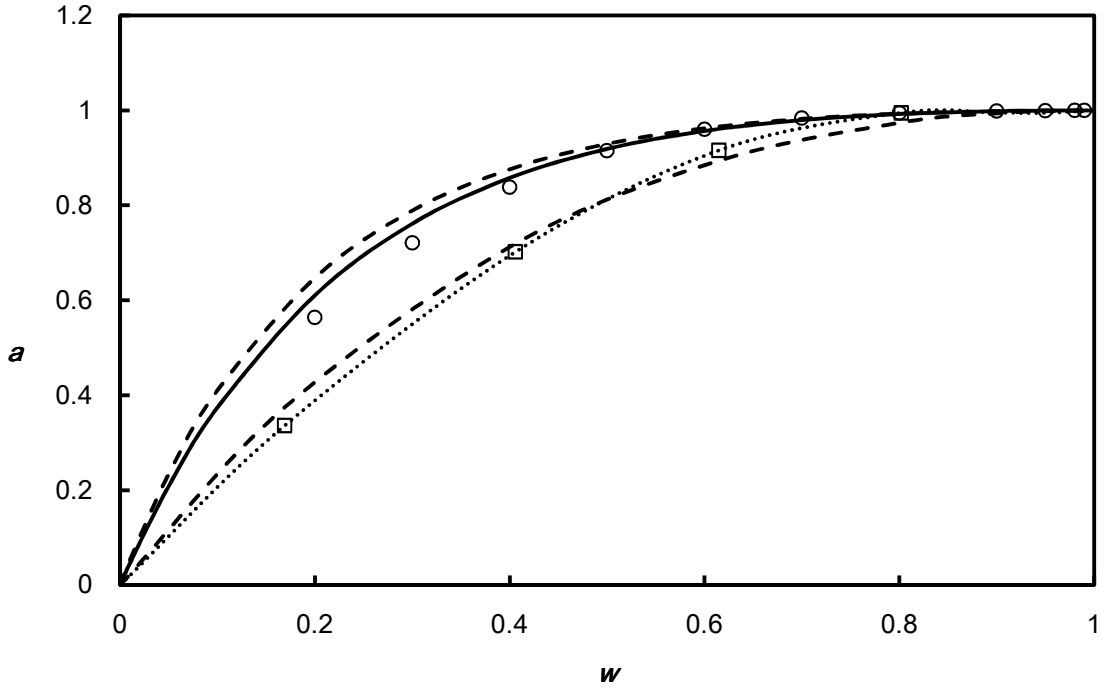

Figure 2. The activity of toluene (circles) in its mixture with polymer PS (Mn=154000 g/mol) and activity of trichloromethane (squares) in its mixture with polymer PS (Mn=90000 g/mol) at 298.15K from experiment[64] (open symbols), COSMO-SAC prediction (solid line for toluene and dotted line for trichloromethane) and COSMO-SAC-FV prediction (dash line).

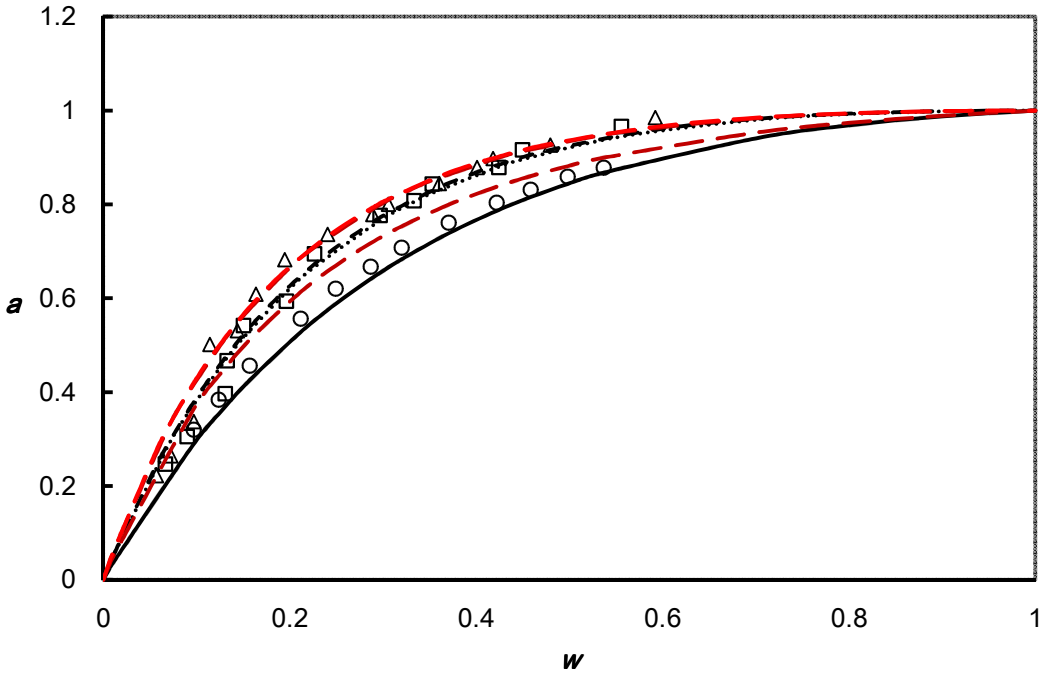

Figure 3. The activity of benzene (circles) in its mixture with polymer PS (Mn=800 g/mol) at 298.15K, (squares) with polymer PS (Mn=20000 g/mol) at 293.15K and (triangles) with polymer PS (Mn=500000 g/mol) at 293.15K from experiment[64] (open symbols), COSMO-SAC prediction (solid line for polymer PS (Mn=800 g/mol), dotted line for polymer PS (Mn=20000 g/mol), dash line for polymer PS (Mn=500000 g/mol)) and COSMO-SAC-FV (red long dash line).

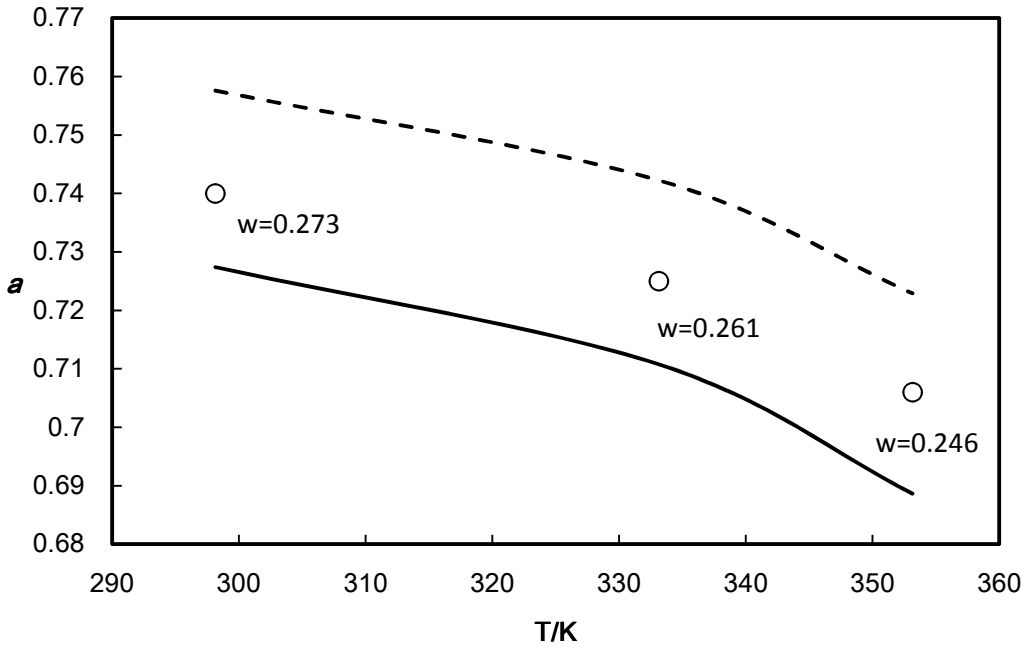

Figure 4. The activity of toluene at different temperatures (T) when mixed with polymer PS (Mn=290000 g/mol) at similar solvent weight fractions (*w*) from experiment[64] (open circles), COSMO-SAC prediction (solid line) and COSMO-SAC-FV prediction (dash line).

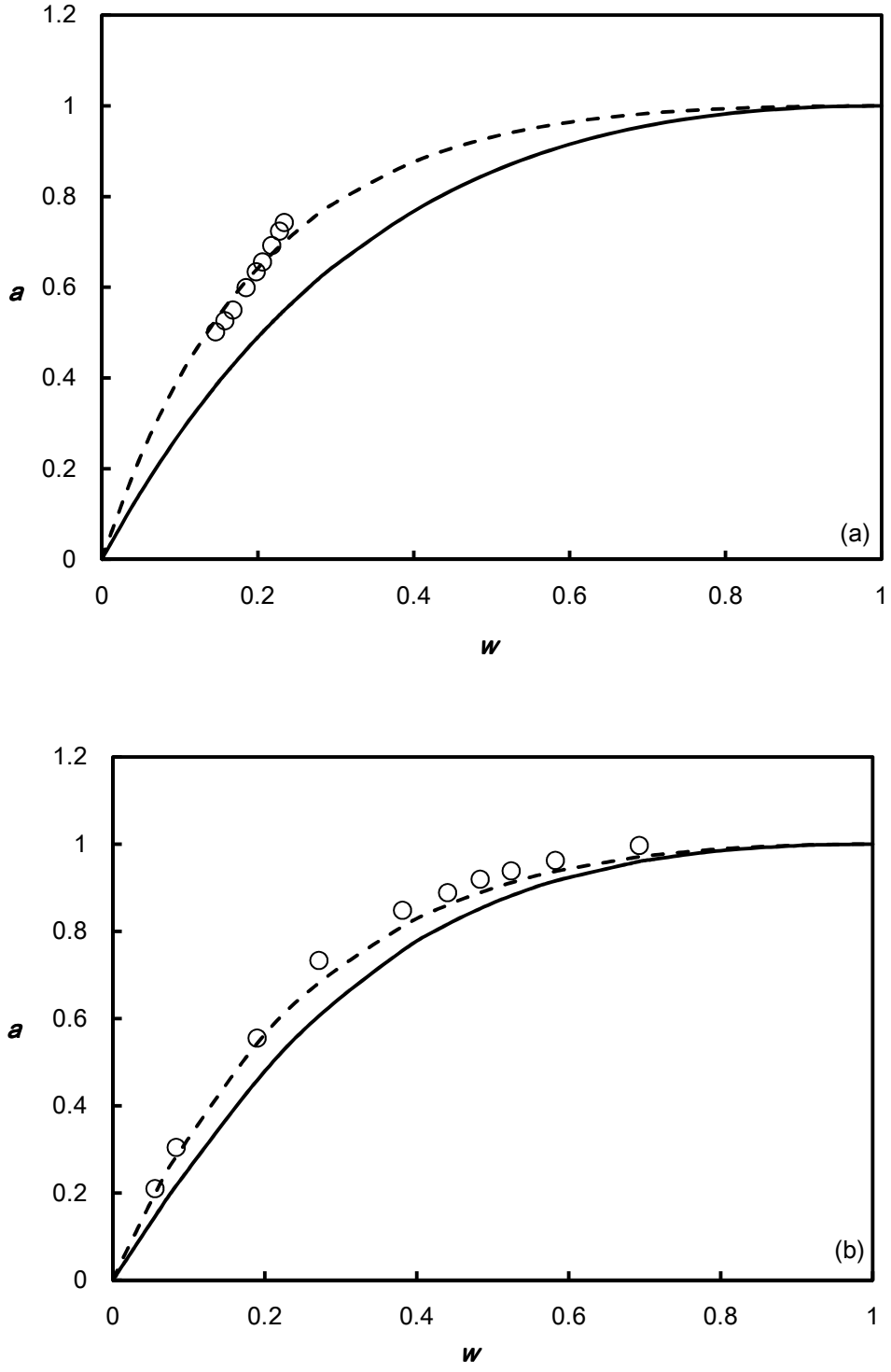

Figure 5. (a) The activity of p-xylene (circles) in its mixture with polymer cis-1,4-PIP (Mn=800000 g/mol) at 293.2K from experiment[84] (open symbols), COSMO-SAC prediction (solid line) and COSMO-SAC-FV prediction (dash line). (b) The activity of tetrahydrofuran

(circles) in its mixture with polymer PVC (Mn=34000 g/mol) at 293.2K from experiment[64] (open symbols), COSMO-SAC prediction (solid line) and COSMO-SAC-FV prediction (dash line).

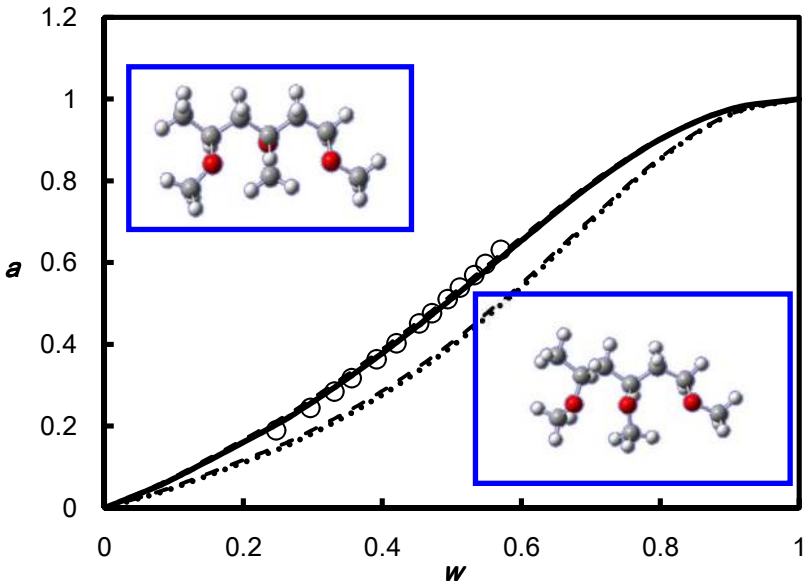

Figure 6. The activity of trichloromethane in its mixture with polymer PVME (Mn=14000 g/mol) at 298.15K from experiment[64] (open circles), COSMO-SAC predictions based on syndiotactic (solid line) and isotactic (dotted line) configurations and COSMO-SAC-FV prediction (dash line). The molecular structures of tri-mer are shown next to the corresponding curves.

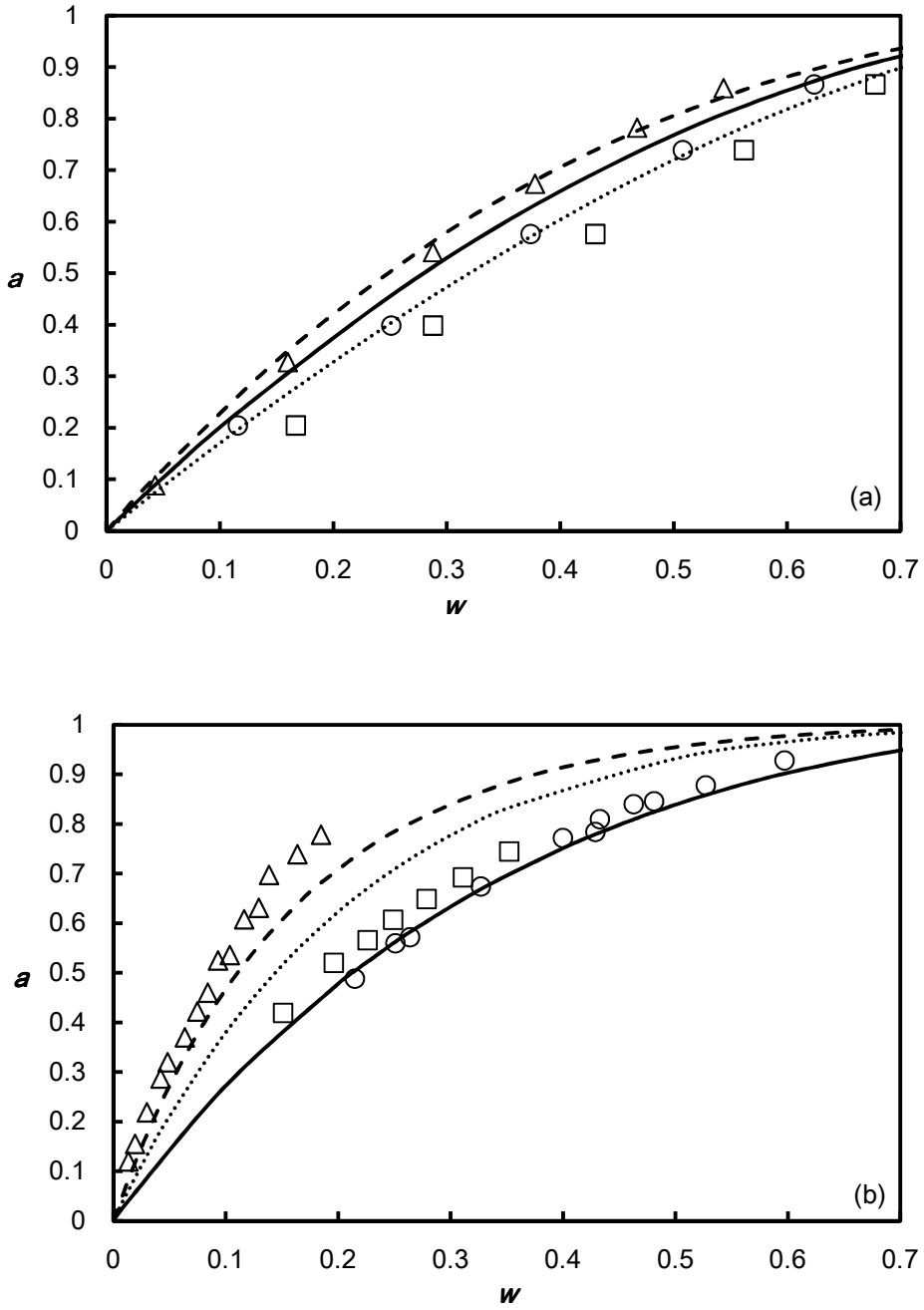

Figure 7. (a) The UCST behavior of cyclohexane in its mixture with polymer PS in different tacticity, PS (Mn=19200 g/mol) (circles), PS (Mn=34900 g/mol) (triangles) and PS (Mn=94300 g/mol) (squares) from experiment (open symbols)[90]; COSMO-SAC-FV predictions (solid line for polymer PS (Mn=19200 g/mol), dotted line for polymer PS (Mn=34900 g/mol), dash line for

polymer PS (Mn=94300 g/mol)) (b) The UCST and LCST behaviors of cyclohexane in its mixture with polymer PaMS (Mn=289200 g/mol) from experiment (circles)[90] and COSMO-SAC-FV prediction (solid lines)

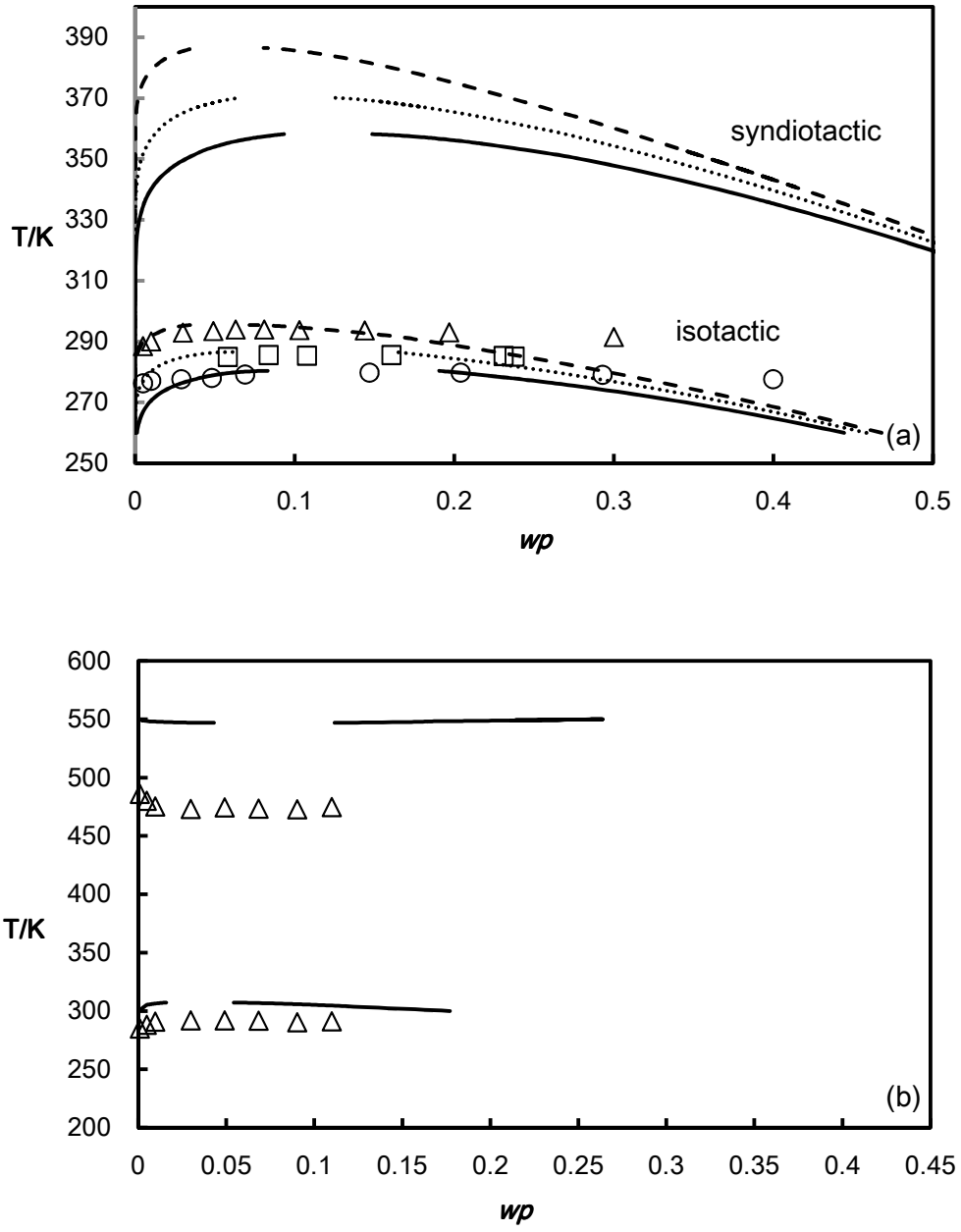

Figure 8. (a) The UCST behavior of cyclohexane in its mixture with polymer PS in different tacticity, PS (Mn=19200 g/mol) (circles), PS (Mn=34900 g/mol) (triangles) and PS (Mn=94300 g/mol) (squares) from experiment (open symbols)[90]; COSMO-SAC-FV

predictions (solid line for polymer PS (Mn=19200 g/mol), dotted line for polymer PS (Mn=34900 g/mol), dash line for polymer PS (Mn=94300 g/mol)) (b) The UCST and LCST behaviors of cyclohexane in its mixture with polymer PaMS (Mn=289200 g/mol) from experiment (circles)[90] and COSMO-SAC-FV prediction (solid lines)